Results in Physics 10 (2018) 155–159

Contents lists available at ScienceDirect

Results in Physics

journal homepage: www.elsevier.com/locate/rinp

Preparation of a novel Mg–Fe master alloy and its spheroidizing effect on graphite in ductile irons

Tong Gao, Zengqiang Li, Junhao Fa, Xiangfa Liu*

Key Laboratory for Liquid–Solid Structural Evolution and Processing of Materials, Ministry of Education, Shandong University, 17923 Jingshi Road, Jinan 250061, PR China

ARTICLE INFO

Keywords:
Mg–Fe master alloy
Ductile iron
Spheroidizing
Graphite particles

ABSTRACT

Spheroidizing treatment is of crucial importance for producing ductile irons. A novel Mg–Fe master alloy has been achieved through the recycling procedure of Al–Si–Fe alloys in this paper. The alloy of Mg–50Fe–16Al–8Si with amounts of block–like Al_2Fe_3Si particles was synthesized by adding Al–14Si–2Fe alloy into Mg melt. It was found that the Mg–Fe master alloy exhibits attractive spheroidizing performance on a ductile iron Q10. This work confirms the significance for achieving Mg–Al and Mg–Fe alloys simultaneously through recycling Al–Si–Fe alloys.

Introduction

The concept of energy saving and materials recycling is widely accepted nowadays [1]. Producing primary electrolytic Al is energy consuming and environment damaging whereas the recycling and reusing of scrap Al is promising [2]. Fe, as an impurity, is common in Al–Si alloys and prefers to form brittle β–Al_5SiFe intermetallic compounds, which is quite harmful for the mechanical properties [3,4]. Based on the theory to modify β–Al_5SiFe or to remove the intermetallic, the methods by overheating the melt, adding neutralized elements, centrifugal separation, and electromagnetic separation have been investigated for decades [5–8]. In our recent work, a new method has been developed by using Mg melt to recycle Al–Si–Fe alloys [9]. During this process, Al and Fe can be separated from β–Al_5SiFe, as a result, Al can be recycled and Fe can be gathered.

Ductile iron is a ferrous metal, which has been widely used in the components of mechanical industries due to its excellent mechanical properties, *e.g.* high strength, toughness and abrasive resistance [10–13]. Except for Fe, the main elements contained in ductile irons are Si and C. Since graphite prefers to exhibit flake–like with sharp edges, easy to cause stress concentration of the matrix, thus spheroidizing treatment is quite important for producing ductile iron [14–16]. Graphite particles can be modified to be sphere–shape through spheroidizing, while the most efficient element to achieve spheroidizing is Mg, and several hypotheses about the spheroidizing mechanism have been put forward [11,17]. In the past decades, purity Mg, RE–Mg alloy and RE–Fe–Si–Mg alloy have been successively used as spheroidizing agents whereas the most applicable method is pour–over treating process [18,19].

As mentioned above, during the recovery process of Al–Si–Fe alloys by the new method, a separation layer containing Mg matrix and high content of Fe can be obtained. By separating the layer, a novel Mg–Fe master alloy was achieved and the microstructure was characterized. Since Mg is beneficial for spheroidizing graphite particles and Fe is easy to dissolve into iron melt, the Mg–Fe master alloy may be applied in ductile irons. Therefore, the ductile iron Q10 was chosen and spheroidizing performance of the Mg–Fe alloy was analyzed.

Experimental

Fig. 1a is the schematic diagram indicating the preparation of Mg–Fe master alloy. First, 400 g Mg was melted to 750 ± 10 °C in a BN ceramic crucible by using resistance furnace under the protection of 1 wt% RJ–2 flux (40–50 wt% $MgCl_2$, 35–45 wt% KCl, 5–8 wt% $BaCl_2$, 5–8 wt% CaF_2, 5–8 wt% NaCl & $CaCl_2$), and 60 g Al–14Si–2Fe alloy was added into the melt. After holding for 30 min, the crucible was transferred into the air and cooled to room temperature. A separation layer, *i.e.* Mg–Fe alloy which will be described later, can be successfully obtained at the bottom. The reason why 750 ± 10 °C and 30 min were chosen as the melting temperature and holding time can be referred in our previous work [9], since under this condition a dense separation layer with Fe–rich particles is easy to be obtained.

The spheroidizing experiments were conducted in a high frequency furnace. Ductile iron Q10 (3.8 wt% C, 1.0 wt% Si, 0.2 wt% Mn, 0.05 wt % S, 0.05 wt% P and Fe balance) with the weight of 200 g was melted in an Al_2O_3 crucible to 1500 ± 30 °C, holding for 5 min. Then the melt

* Corresponding author.
E-mail address: xfliu@sdu.edu.cn (X. Liu).

https://doi.org/10.1016/j.rinp.2018.05.035
Received 28 April 2018; Received in revised form 17 May 2018; Accepted 19 May 2018
Available online 28 May 2018

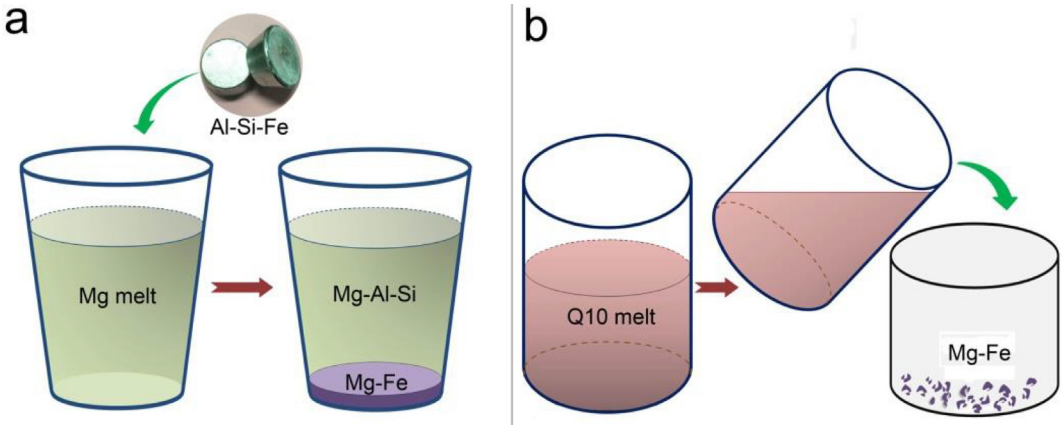

Fig. 1. Schematic diagram showing the preparation of Mg–Fe master alloy (a) and the spheroidizing experiment on Q10 (b).

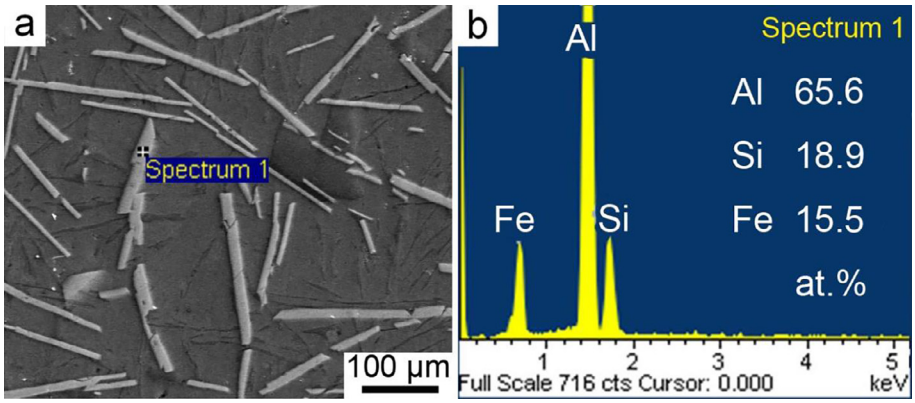

Fig. 2. Microstructure (a) and EDX (b) of β–Al_5FeSi in Al–14Si–2Fe alloy.

was poured into a mould with pre–heated Mg–Fe master alloy (Fig. 1b). During the following solidification procedure, the Mg–Fe master alloy melted and performed spheroidizing effect on the graphite particles in Q10 alloy.

The samples were cut from the cooled ingots then mechanically grinded by SiC metallographic sandpaper. After that, the samples were polished using Cr_2O_3 turbid liquid (5%) for Al–14Si–2Fe alloy and Q10, and using MgO turbid liquid (5%) for Mg–Fe master alloy by a polishing machine. The microstructure observation and analysis were carried out by a Leica DM2700 High–Scope Video Microscope (HSVM) and a Hitachi SU–70 field emission scanning electron microscopy (FESEM) operated at 15 kV and linked with an energy dispersive X–ray spectrometry (EDX) attachment. Image J software was used to characterize the area fraction, size distribution and aspect ratio (AR) of the graphite particles.

Results and discussions

Fig. 2 shows the microstructure and EDX of the Al–14Si–2Fe alloy. It was found that the primary Fe–rich intermetallics are β–Al_5FeSi, exhibiting flake–like. The nominal atomic ratio between Al and Fe in the β–Al_5FeSi phase is up to 5:1, thus a large proportion of Al atoms are bounded by Fe atoms and can hardly be recovered by traditional methods. Using the above method, *i.e.* introducing the Al–14Si–2Fe alloy into Mg melt, a separation layer was obtained in the cooled ingot, as shown in Fig. 3a and b. Through this process, β–Al_5FeSi evolves to a Fe-rich phase and settles to the bottom of the melt, which is mainly due to the density difference between Mg melt and the Fe–rich particles as similarly reported in [9,20]. As a result, Mg–Al alloy can be obtained at the top of the ingot while Mg–Fe alloy can be achieved at the bottom part. Fig. 3d displays the microstructure of the separation layer and amounts of block–like Fe–rich intermetallics have formed, which is quite different from the flake–like β–Al_5FeSi. EDX result (Fig. 3c) indicates that the block–like particles can be approximately expressed by the formula Al_2Fe_3Si. This phase has a much lower content of Al indicating that a greater proportion of Al has been released to Mg melt by β–Al_5FeSi and thus can be recycled. This is also the key point of recycling scrap Al–Si–Fe alloys by this method, and Mg–Al and Mg–Fe alloys can be obtained simultaneously.

It is necessary to mention that since no standard samples with high Fe–content Mg alloys can be referred, therefore the composition of the Mg–Fe master alloy cannot be accurately detected by spectrometer machines. However, the Al and Fe content in the upper Mg–Al alloy was detected to be 11.723 wt% and 0.015 wt% respectively, also indirectly indicating that this method is efficient to gather Fe–rich particles in the bottom. Besides, the statistic area fraction of Al_2Fe_3Si in the bottom part can be measured by Image J software (Fig. 3e), which is 42.3%. Based on the density of Mg and Al_2Fe_3Si particles [21], the Mg–Fe master alloy can be roughly calculated to be Mg–50Fe–16Al–8Si (wt.%).

To check spheroidizing performance of the Mg–Fe master alloy,

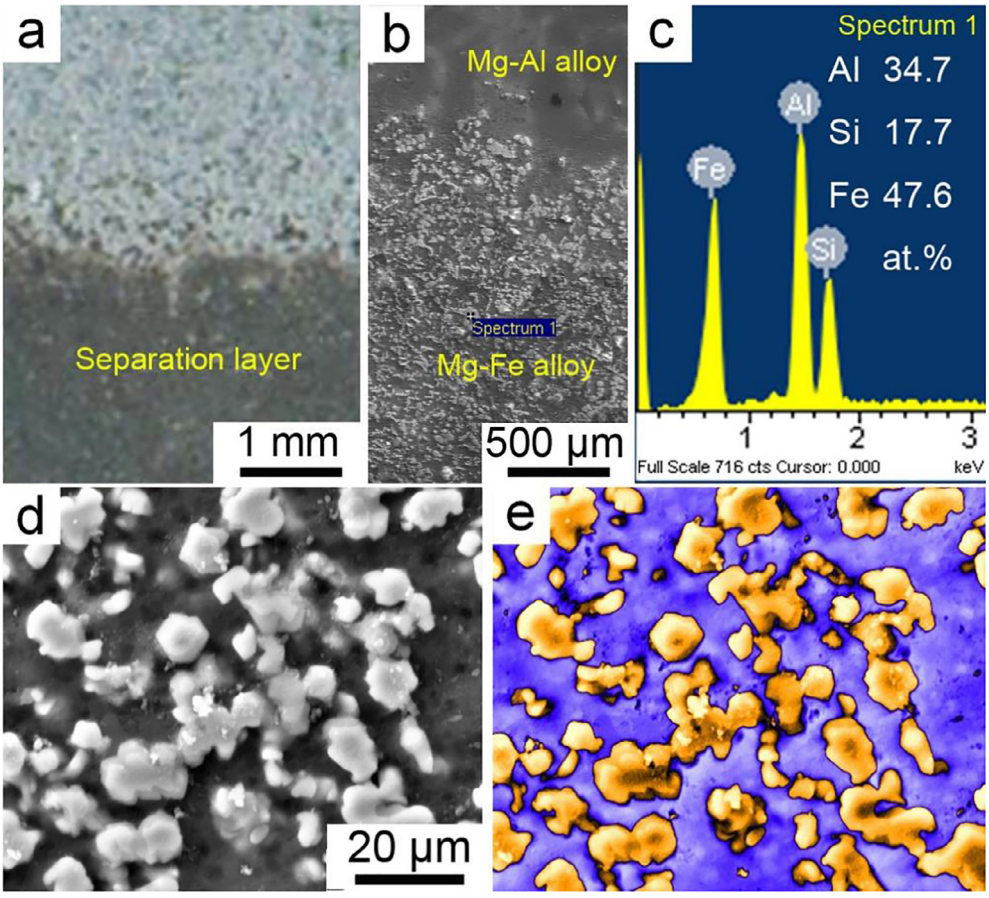

Fig. 3. (a, b) The bottom part of the cooled ingot, showing the separation layer; (c) EDX of the Fe–rich particles in the separation layer; (d) Microstructure of Al_2Fe_3Si phase in the separation layer; (e) The colored image of (d) by using Image J software to calculate the volume fraction of Al_2Fe_3Si.

experiments on ductile iron Q10 were conducted. Fig. 4a is the microstructure of raw Q10, in which the graphite particles exhibit irregular. Using Image J to clearly distinguish the matrix and graphite particles (Fig. 4b), the AR of the graphite particles can be obtained. Fig. 4c is the histogram showing the distribution of AR through analyzing more than 400 particles. It indicates that the AR values of most graphite particles are far away from 1.0, *i.e.* the raw alloy has no spheroidizing performance before adding Mg–Fe alloy.

With the addition of 0.5 wt% Mg–Fe master alloy into Q10 melt, the obtained microstructure is shown in Fig. 5a. Fig. 5b and c show the statistic of the diameters and the AR of graphite particles, respectively. It can be found that most of the graphite particles exhibit sphere–like (Fig. 5a), confirmed by the AR histogram (Fig. 5c). From Fig. 5b, the average size of the graphite particles is calculated to be 0.9 μm.

Fig. 6a, b and c are the corresponding microstructures of Q10 when the addition of Mg–Fe master alloy is increased to 1.0 wt%. It was found that the graphite particles have smaller average size, which is about 0.6 μm (Fig. 6a and b). The histogram in Fig. 6c obviously indicates that the particles are approximate perfect sphere shape.

Based on above results, it can be seen that the novel Mg–Fe master alloy performs attractive spheroidizing effect on Q10. Therefore, through the method for Al–Si–Fe recovering shown in Fig. 1a, the finally obtained Mg–Al alloy at upper part can be used to produce Mg alloys or act as master alloys in Al industries, while the Mg–Fe master alloy at the bottom part can exhibit spheroidizing effect in ductile irons. Compared with traditional spheroidizing agents, the preparation of Mg–Fe master alloy is material saving and energy saving. However, it is still necessary to mention that since impurities in Al–Si–Fe alloys may affect the separation performance of Al and Fe by this method, therefore detailed work revealing the effect of Mn, P, Cr, *etc.*, should be carried out in the further study. These impurities may also directly affect the spheroidizing efficiency of the Mg–Fe master alloy. Besides, related equipment to achieve melt separation is also needed for promoting its application in industries in the future.

Conclusions

A novel Mg–Fe master alloy has been prepared in this paper along with the recycling process of scrap Al–Si–Fe alloys. An alloy of Mg–50Fe–16Al–8Si with amounts of block–like Al_2Fe_3Si has been obtained, which has been proven to exhibit obvious spheroidizing performance on graphite particles in ductile iron Q10. With 1% addition of the Mg–50Fe–16Al–8Si master alloy, the average size of the graphite particles in Q10 can be lower to 0.6 μm.

Acknowledgements

This research was financially supported by the National Natural Science Foundation of China (No. 51601106), China Postdoctoral Science Foundation (No. 2017T100489), and Special Fund for Postdoctoral Innovation Project of Shandong Province (No. 201701010).

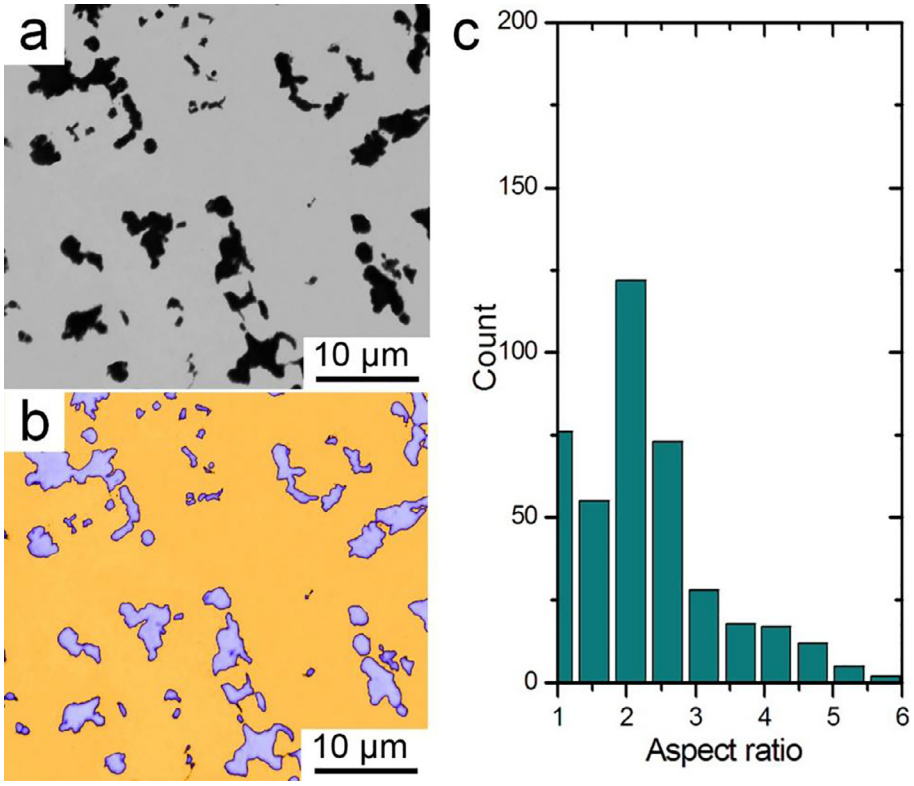

Fig. 4. (a) Microstructure of cast iron Q10, indicating the morphology of graphite particles; (b) The image of (a) processed by Image J software; (c) The histogram of aspect ratio by analyzing graphite particles.

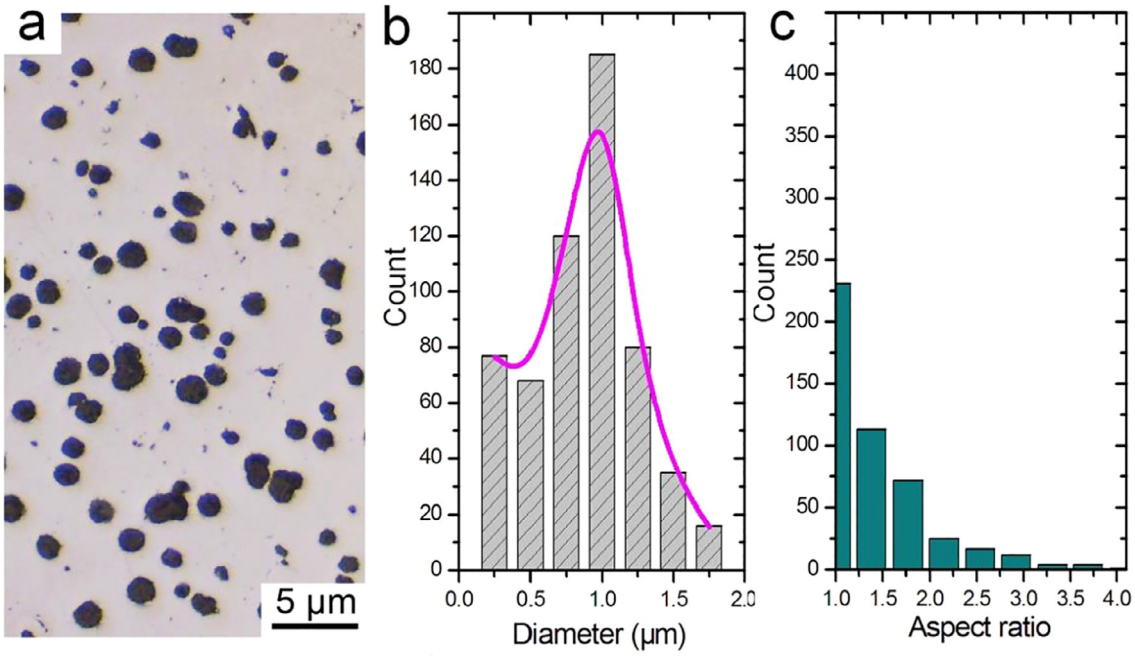

Fig. 5. (a) Microstructure of Q10 alloy spheroidized by 0.5 wt% of Mg–Fe master alloy; (b) Histograms of graphite particles' diameter; (c) Aspect ratio of graphite particles' diameter.

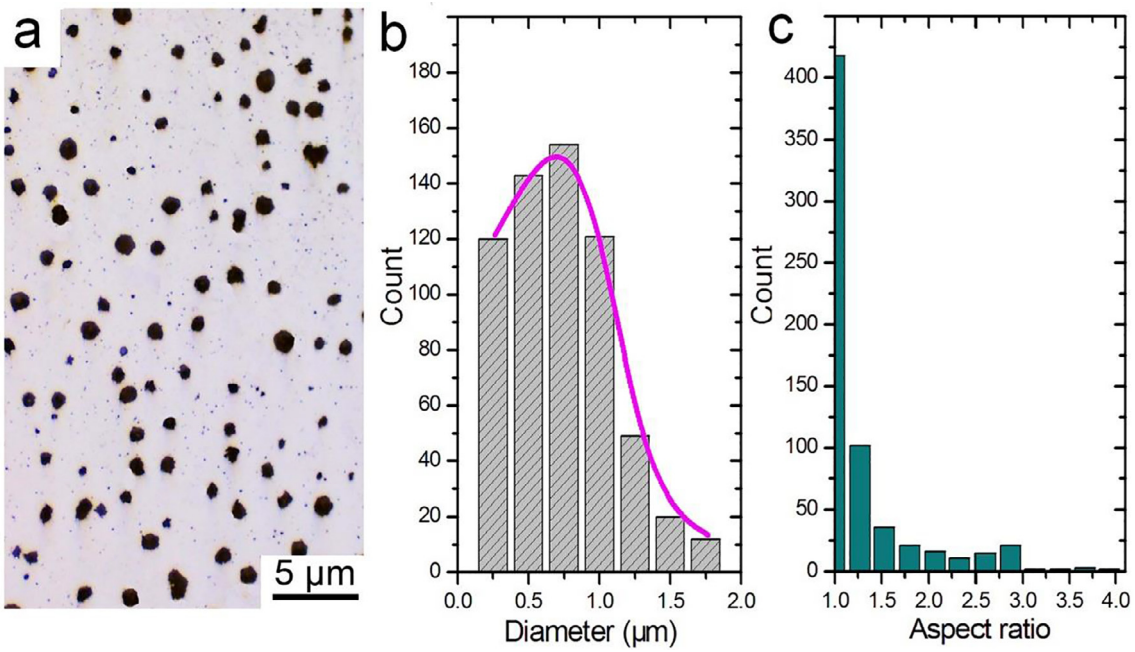

Fig. 6. (a) Microstructure of Q10 alloy spheroidized by 1.0 wt% of Mg–Fe master alloy; (b) Histograms of graphite particles' diameter; (c) Aspect ratio of graphite particles' diameter.

References

[1] Fysikopoulos A, Anagnostakis D, Salonitis K, Chryssolouris G. An empirical study of the energy consumption in automotive assembly. Proc Cirp 2012;3:477–82.

[2] Zhang YL, Sun MX, Hong JL, Han XF, He J, Shi WX, Li XZ. Environmental footprint of aluminum production in China. J Clean Prod 2016;133:1242–51.

[3] Yu JM, Wanderka N, Miehe G, Banhart J. Intermetallic phases in high purity Al–10Si–0.3Fe cast alloys with and without Sr modification studied by FIB tomography and TEM. Intermetallics 2016;72:53–61.

[4] Goudar DM, Raju K, Srivastava VC, Rudrakshi GB. Effect of copper and iron on the wear properties of spray formed Al–28Si alloy. Mater Des 2013;51:383–90.

[5] Alizadeh M, Karamouz M. Effect of periodic melt shearing process and cooling rate on structure and hardness of Al–0.7Fe aluminum alloy. Mater Des 2014;55:204–11.

[6] Kim HY, Park TY, Han SW, Lee HM. Effects of Mn on the crystal structure of α–Al(Mn, Fe)Si particles in A356 alloys. J Cryst Growth 2006;291:207–11.

[7] Basak CB, Hari Babu N. Morphological changes and segregation of β–$Al_9Fe_2Si_2$ phase: a perspective from better recyclability of cast Al–Si alloys. Mater Des 2016;108:277–88.

[8] Nafisia S, Emadib D, Shehatab MT, Ghomashchi R. Effects of electromagnetic stirring and superheat on the microstructural characteristics of Al–Si–Fe alloy. Mater Sci Eng A 2006;432:71–83.

[9] Gao T, Li ZQ, Zhang YX, Qin JY, Liu XF. Evolution of Fe–rich phases in Mg melt and a novel method for separating Al and Fe from Al–Si–Fe alloys. Mater Des 2017;134:71–80.

[10] Rebasa N, Dommarco R, Sikora J. Wear resistance of high nodule count ductile iron. Wear 2002;253:855–61.

[11] Zimba J, Samandi M, Yu D, Chandra T, Navara E, Simbi DJ. Un–lubricated sliding wear performance of unalloyed austempered ductile iron under high contact stresses. Mater Des 2004;25:431–8.

[12] Ceccarelli B, Dommarco R, Martinez R, Gamba M. Abrasion and impact properties of partially chilled ductile iron. Wear 2004;256:49–55.

[13] Eric O, Sidjanin L, Miskovic Z, Zec S, Jovanovic M. Microstructure and toughness of Cu–Ni–Mo austempered ductile iron. Mater Lett 2004;58:2707–11.

[14] Shepperson S, Allen C. The abrasive wear behaviour of austempered spheroidal cast iron. Wear 1988;121:271–87.

[15] Di H, Zhang X, Wang G, Liu X. Spheroidizing kinetics of eutectic carbide in the twin roll–casting of M2 high–speed steel. J Mater Process Tech 2005;166:359–63.

[16] Zhu GH, Zheng G. Directly spheroidizing during hot deformation in GCr15 steels. Front Mater Sci China 2008;2:72–5.

[17] Elsayed AH, Megahed MM, Sadek AA, Abouelela KM. Fracture toughness characterization of austempered ductile iron produced using both conventional and two–step austempering processes. Mater Des 2009;30:1866–77.

[18] Duan J, Jiang Z, Fu H. Effect of RE–Mg complex modifier on structure and performance of high speed steel roll. J Rare Earth 2007;25:259–63.

[19] Xu C. On the threshold value Δk_(th) of rare earth–magnesium ductile iron. Acta Metall. Sin. 1981;17:661–6.

[20] Gao T, Li ZQ, Zhang YX, Liu XF. Evolution behavior of γ–$Al_{3.5}$FeSi in Mg melt and a separation method of Fe from Al–Si–Fe alloys. Acta Metall Sin (Engl Lett) 2018;31:48–54.

[21] Materials Data JADE Release 5, XRD Pattern Processing and Materials Data Inc. (MDI), 2002.